

LETTER • OPEN ACCESS

## ENSO modulation of summertime tropospheric ozone over China

To cite this article: Yang Yang *et al* 2022 *Environ. Res. Lett.* **17** 034020

View the [article online](#) for updates and enhancements.

### You may also like







- [Impacts of sectoral emissions in China and the implications: air quality, public health, crop production, and economic costs](#)  
Y Gu, T W Wong, C K Law et al.
- [Reduced health burden and economic benefits of cleaner fuel usage from household energy consumption across rural and urban China](#)  
Chenxi Lu, Shaohui Zhang, Chang Tan et al.
- [Interannual variations of the influences of MJO on winter rainfall in southern China](#)  
Xiong Chen, Chongyin Li, Lifeng Li et al.

ENVIRONMENTAL RESEARCH  
LETTERS

## LETTER

## ENSO modulation of summertime tropospheric ozone over China

## OPEN ACCESS

Yang Yang<sup>1,\*</sup> , Mengyun Li<sup>1</sup>, Hailong Wang<sup>2</sup> , Huimin Li<sup>1</sup>, Pinya Wang<sup>1</sup> , Ke Li<sup>1</sup> , Meng Gao<sup>3</sup>   
and Hong Liao<sup>1</sup> RECEIVED  
22 October 2021REVISED  
9 February 2022ACCEPTED FOR PUBLICATION  
14 February 2022PUBLISHED  
24 February 2022

Original content from  
this work may be used  
under the terms of the  
[Creative Commons  
Attribution 4.0 licence](https://creativecommons.org/licenses/by/4.0/).

Any further distribution  
of this work must  
maintain attribution to  
the author(s) and the title  
of the work, journal  
citation and DOI.



<sup>1</sup> Jiangsu Key Laboratory of Atmospheric Environment Monitoring and Pollution Control, Jiangsu Collaborative Innovation Center of Atmospheric Environment and Equipment Technology, School of Environmental Science and Engineering, Nanjing University of Information Science and Technology, Nanjing, Jiangsu, People's Republic of China

<sup>2</sup> Atmospheric Sciences and Global Change Division, Pacific Northwest National Laboratory, Richland, WA, United States of America

<sup>3</sup> Department of Geography, State Key Laboratory of Environmental and Biological Analysis, Hong Kong Baptist University, Hong Kong SAR, People's Republic of China

\* Author to whom any correspondence should be addressed.

E-mail: [yang.yang@nuist.edu.cn](mailto:yang.yang@nuist.edu.cn)

**Keywords:** O<sub>3</sub>, China, El Niño, ENSO

Supplementary material for this article is available [online](#)

**Abstract**

Ozone (O<sub>3</sub>) is one of the most critical pollutants affecting air quality in China in recent years. In this study, different impacts of the El Niño–Southern Oscillation (ENSO) warm/cold phases on summertime tropospheric O<sub>3</sub> over China are examined based on model simulations, ground measurements, and reanalysis data. Summertime surface O<sub>3</sub> concentrations in China show a positive correlation with ENSO index during years 1990–2019, with the largest increases by 20% over southern China in El Niño (warm phase) relative to La Niña (cold phase) years. The ENSO modulation extends to the middle and even upper troposphere. Our analysis indicates that O<sub>3</sub> flux convergence associated with weakened southerlies is the primary reason for the increase in tropospheric O<sub>3</sub> over southern China. In addition, the O<sub>3</sub> increase during El Niño years is mainly from domestic emissions in China. This study highlights the potential significance of ENSO in modulating tropospheric O<sub>3</sub> concentrations in China, with great implications for O<sub>3</sub> pollution mitigation.

**1. Introduction**

Tropospheric ozone (O<sub>3</sub>) is now the most critical air pollutant in China apart from particulate matter in recent years (Fu *et al* 2019, Gao *et al* 2020, Li *et al* 2021). In the recent decade, daily maximum 8 h average (MDA8) O<sub>3</sub> concentration in China in the warm season increased at a rate of 5% per year, which is faster than any other regions of the world (Lu *et al* 2018, 2020). Tropospheric O<sub>3</sub> is produced through the oxidation of carbon monoxide (CO) and volatile organic compounds (VOCs) with the sunlight in the existence of nitrogen oxides (NO<sub>x</sub>). High O<sub>3</sub> concentration harms human health (Jerrett *et al* 2009, Malley *et al* 2017) and reduces crop yields (Yue *et al* 2017, Mills *et al* 2018). Therefore, it is of great significance to understand factors that modulate the variation of O<sub>3</sub> concentrations in China.

In addition to anthropogenic emissions of precursor gases (Qu *et al* 2020) and atmospheric

oxidation capacity (Lu *et al* 2019a), meteorological conditions also exert various impacts on O<sub>3</sub> concentrations (Yin *et al* 2019). High temperature along with intense solar radiation enhances both photochemical reactions and natural precursor emissions of O<sub>3</sub> (Jacob and Winner 2009). Thus, O<sub>3</sub> pollution is generally severe in summer with strong sunlight. Relative humidity (RH) is negatively correlated with O<sub>3</sub> concentration due to the strong uptake of O<sub>3</sub> by trees under high RH conditions (Kavassalis and Murphy 2017) and water vapor from marine air also serves as a chemical sink of O<sub>3</sub> at low NO<sub>x</sub> conditions (Lu *et al* 2018). The existence of clouds can reduce O<sub>3</sub> concentrations via decreasing the solar radiation and hence photochemical reactions (Jeong and Park 2013). Through changing the air stagnant condition and atmospheric transport, winds influence O<sub>3</sub> concentrations in both local and downwind areas (Doherty *et al* 2013, Zhang *et al* 2017). Gong *et al* (2019) revealed that O<sub>3</sub> pollution events in

northern China occurred with high temperature, low RH, an anomalous high in the mid-troposphere, and downdraft in the lower troposphere. Changes in meteorological conditions are strongly associated with large-scale atmospheric circulation anomalies. Yang *et al* (2014) found that the year-by-year changes in the East Asian summer monsoon strength caused an interannual variation in near-surface O<sub>3</sub> concentrations over central-eastern China by 2%–5%, attributed to the changing transboundary transport of O<sub>3</sub>, with high O<sub>3</sub> levels appearing in strong monsoon years. A stronger western Pacific subtropical high can bring in more humid air, resulting in more clouds and lower temperature in southern China, which decreases O<sub>3</sub> concentrations there (Zhao and Wang 2017, Yin *et al* 2019).

El Niño–Southern Oscillation (ENSO) is the dominant mode of variability in Earth's climate system at interannual time scales (Ropelewski and Halpert 1987). It features anomalous high sea surface temperatures (SSTs) over the tropical eastern Pacific Ocean during the warm phase (i.e. El Niño) and anomalous low SST during the cold phase (i.e. La Niña). ENSO can influence atmospheric circulations and weather conditions across the globe and further change global O<sub>3</sub> distributions. Numerous studies have examined the ENSO influences on tropical O<sub>3</sub> (e.g. Oman *et al* 2011, Xie *et al* 2014, Olsen *et al* 2016) and the transpacific transport of O<sub>3</sub> (Lin and McElroy 2010, Xue *et al* 2021).

Although ENSO signal weakens in boreal summer season, when an ENSO event is developing, until its mature phase in boreal winter of the year, ENSO has been reported to have remarkable impacts on summertime O<sub>3</sub> in the mid-latitudes of the Northern Hemisphere (Zhang *et al* 2015, Shen and Mickley 2017, Xu *et al* 2017, Wie *et al* 2021). Based on surface ozone observations and meteorological variables from reanalysis data, Xu *et al* (2017) found that surface O<sub>3</sub> concentrations decreased during El Niño and increased during La Niña years (including summer) over the continental United States over 1993–2013, which was attributed to ENSO-induced changes in chemical processes and dynamic transport. Shen and Mickley (2017) also reported an El Niño–O<sub>3</sub> connection in eastern United States and found that El Niño reduced moisture transport into the Atlantic coast states but enhanced moisture flux into the south-central states, leading to surface O<sub>3</sub> increases and decreases, respectively, over these two regions in summer. Zhang *et al* (2015) investigated the influence of ENSO on the total O<sub>3</sub> column (TOC) in China using satellite data and found that summertime TOC increased over northeastern and northwestern China during El Niño events, while it decreased over southern and southwestern China as well as in the middle reach of the Yellow River during La Niña events. Based

on satellite measurements and chemistry-climate model simulations, Wie *et al* (2021) examined the variability of tropospheric column O<sub>3</sub> over East Asia and found that that O<sub>3</sub> increased in the troposphere 4–5 months after the La Niña peak, associated with anomalous O<sub>3</sub> transport from higher latitudes. However, few studies have quantified the roles of different physical and chemical processes in determining the impact of ENSO on summertime O<sub>3</sub> variability in China. In addition, ENSO-driven O<sub>3</sub> changes near the surface in China, which is more directly linked to air quality and human health than the total column burden, were rarely studied in previous works.

In this study, the impact of ENSO on summertime tropospheric O<sub>3</sub> concentrations in China and its mechanisms are investigated using global chemical transport model simulations over 1990–2019 driven by meteorological fields from reanalysis data. Details of the model and experimental design are described in section 2. Section 3 quantifies the influence of ENSO on near-surface O<sub>3</sub> concentrations in China. The mechanisms behind the impacts are analyzed in section 4. Section 5 summarizes the main results and discusses potential uncertainties in this study and implications for future studies.

## 2. Methods

### 2.1. Model description

O<sub>3</sub> concentrations are simulated in this study by using GEOS-Chem model v12.9.3 with a horizontal resolution of 2° latitude × 2.5° longitude and 47 vertical layers from the surface to 0.01 hPa. GEOS-Chem is a global model of atmospheric chemistry with fully coupled O<sub>3</sub>–NO<sub>x</sub>–hydrocarbon–aerosol chemical mechanisms (Pye *et al* 2009, Mao *et al* 2013, Sherwen *et al* 2016). The boundary layer mixing is represented by a nonlocal scheme (Lin and McElroy 2010) and the stratospheric O<sub>3</sub> chemistry uses the LINOZ scheme (McLinden *et al* 2000). Meteorological fields driving the model in this study are from NASA Modern-Era Retrospective analysis for Research and Applications, Version 2 (MERRA-2). Additionally, the geopotential height data from the National Center for Environmental Prediction and National Center for Atmospheric Research reanalysis are used in our analysis due to the lack of geopotential heights in the MERRA-2 reanalysis products. The tendencies of different chemical and physical processes of tracers are written out from GEOS-Chem, which can be used to quantify the relative contribution of individual processes to variations in O<sub>3</sub> concentrations.

### 2.2. Emissions

Global baseline anthropogenic emissions utilized in this study are obtained from the community

emissions data system (Hoesly *et al* 2018) and biomass burning emissions are from the Global Fire Emissions Database version 4 (van der Werf *et al* 2017). Anthropogenic emissions of O<sub>3</sub> precursor gases, including CO, NO<sub>x</sub> and VOCs, in China are replaced with the MEIC (Multi-resolution Emissions Inventory) emission inventory, which is a national emission inventory for China and includes emissions from transportation, residential, industry and power plants (Zheng *et al* 2018). Biogenic emissions are estimated with the Model of Emissions of Gases and Aerosols from Nature version 2.1 (Guenther *et al* 2012). GEOS-Chem simulations of surface O<sub>3</sub> in China using the same emission configurations have been extensively evaluated in previous studies (e.g. Ni *et al* 2018, Li *et al* 2019, Lu *et al* 2019b) and the model showed good skills in reproducing observed O<sub>3</sub> concentrations and spatial distribution in China.

### 2.3. Experiments

In this study, O<sub>3</sub> concentrations are estimated for years 1990–2019 in the baseline simulation (BASE) using the GEOS-Chem model driven by MERRA-2 meteorological fields. In order to quantify the impact of ENSO on O<sub>3</sub> in China, the effect from emission changes is removed by keeping anthropogenic, biomass burning and natural emissions at their year 2017 level in the BASE simulation. But we note that the year-to-year emissions are different and choosing 2017 as the base year may cause a small bias in the ENSO influence in magnitude. The quantitative impact of ENSO on the interannual variation of summertime O<sub>3</sub> in China can be obtained from the BASE experiment. Unless specified otherwise, results in this study are derived from the BASE experiment. Another sensitivity simulation, which is same as BASE but with anthropogenic emissions of O<sub>3</sub> precursors (CO, NO<sub>x</sub> and VOCs) from China turned off (NO\_CHN), is also conducted to understand the role of China domestic emissions in the ENSO-induced O<sub>3</sub> variation by differing the two simulations (BASE–NO\_CHN).

### 2.4. ENSO index

The Niño 3.4 index is employed to characterize the phase and intensity of ENSO events. It is calculated as the area averaged SST anomaly within the region of 5° S–5° N and 170–120° W based on MERRA-2 reanalysis in this study. Niño 3.4 index averaged over June–July–August (JJA) is used to explore the relationship between ENSO and O<sub>3</sub> in China during the boreal summer.

## 3. Impact of ENSO on the interannual variation in O<sub>3</sub> over China

To investigate the connection between ENSO and summertime O<sub>3</sub> in China, the empirical orthogonal

function (EOF) analysis of GEOS-Chem JJA near-surface O<sub>3</sub> concentrations is conducted. As shown in figure S1(a) (available online at [stacks.iop.org/ERL/17/034020/mmedia](https://stacks.iop.org/ERL/17/034020/mmedia)), the leading EOF can explain 23% of interannual variability of near-surface O<sub>3</sub> concentrations in Asia and positive pattern of EOF appears in the whole China, especially over southern China. The principal component (PC) of the leading EOF of near-surface O<sub>3</sub> concentrations is positively correlated with the JJA mean Niño 3.4 index (figure S1(b)). The correlation coefficient between the leading PC and Niño 3.4 index is +0.5 and statistically significant at a 99% confidence level, indicating that ENSO may play a vital role in the interannual variations in JJA near-surface O<sub>3</sub> concentrations in southern China, although note that the leading-mode EOF only explains 23% of the O<sub>3</sub> variance over China.

The spatial distribution of the correlation coefficients between the simulated JJA mean near-surface O<sub>3</sub> concentrations and Niño 3.4 index over 1990–2019 is shown in figure 1(a) to further illustrate the relationship between ENSO and O<sub>3</sub> in China. Statistically significant and positive correlation coefficients are shown in southern China, part of Yangtze River Delta, part of northeastern China, and the Tibetan Plateau. Since ENSO has a detectable impact on the interannual variation of near-surface O<sub>3</sub> concentrations in China, particularly in southern China among all regions based on the EOF analysis, we mainly focus on the O<sub>3</sub> variations in southern China (97.5–117.5° E, 20–32° N) influenced by ENSO. Simulated near-surface O<sub>3</sub> concentrations averaged over southern China present a positive correlation with ENSO index, with statistically significant correlation coefficient between O<sub>3</sub> and Niño 3.4 index of +0.55 at a 99% confidence level. That is, El Niño (La Niña) is accompanied by an increase (decrease) in near-surface O<sub>3</sub> concentrations over southern China in summer.

Note that, there are two types of ENSO, eastern Pacific (EP) type and central Pacific (CP) type (Kao and Yu 2009). We also calculated the correlation coefficient (R) between EP/CP Index based on Kao and Yu (2009) and O<sub>3</sub> concentrations in southern China (figure S2). CP Index is positively correlated with O<sub>3</sub> (R = 0.30), while EP Index does not have discernable correlation (0.03). Considering the higher frequency of CP El Niño events in recent decades relative to past centuries (Freund *et al* 2019), ENSO could be more influential on O<sub>3</sub> in China. We also tested the Niño 1 + 2 (0.21), Niño 3 (0.50) and Niño 4 (0.52) Indices and found that all the correlation coefficients between these indices and O<sub>3</sub> are lower than Niño 3.4 (0.55). ENSO may have a cross-correlation with O<sub>3</sub> (Shen *et al* 2017). The correlations between January–February–March/March–April–May mean Niño 3.4

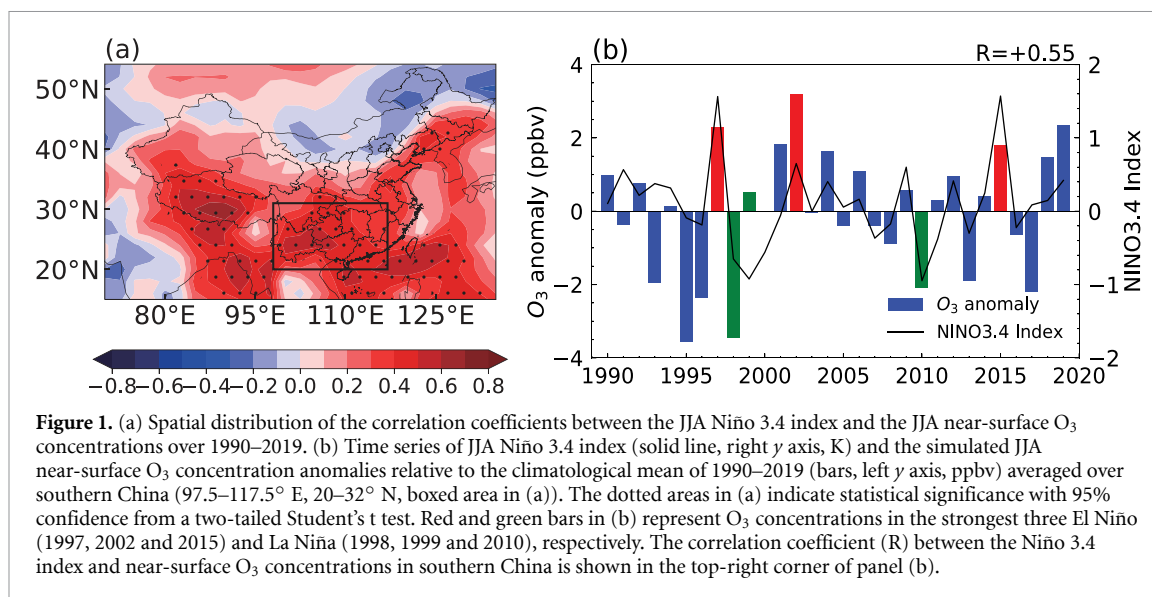


**Figure 1.** (a) Spatial distribution of the correlation coefficients between the JJA Niño 3.4 index and the JJA near-surface  $O_3$  concentrations over 1990–2019. (b) Time series of JJA Niño 3.4 index (solid line, right y axis, K) and the simulated JJA near-surface  $O_3$  concentration anomalies relative to the climatological mean of 1990–2019 (bars, left y axis, ppbv) averaged over southern China ( $97.5^{\circ}\text{E}$ – $117.5^{\circ}\text{E}$ ,  $20^{\circ}\text{N}$ – $32^{\circ}\text{N}$ , boxed area in (a)). The dotted areas in (a) indicate statistical significance with 95% confidence from a two-tailed Student's *t* test. Red and green bars in (b) represent  $O_3$  concentrations in the strongest three El Niño (1997, 2002 and 2015) and La Niña (1998, 1999 and 2010), respectively. The correlation coefficient (*R*) between the Niño 3.4 index and near-surface  $O_3$  concentrations in southern China is shown in the top-right corner of panel (b).

and JJA  $O_3$  concentrations over southern China are also estimated and they only present weak negative relationships, with a correlation coefficient of  $-0.26$  and  $-0.10$ , respectively.

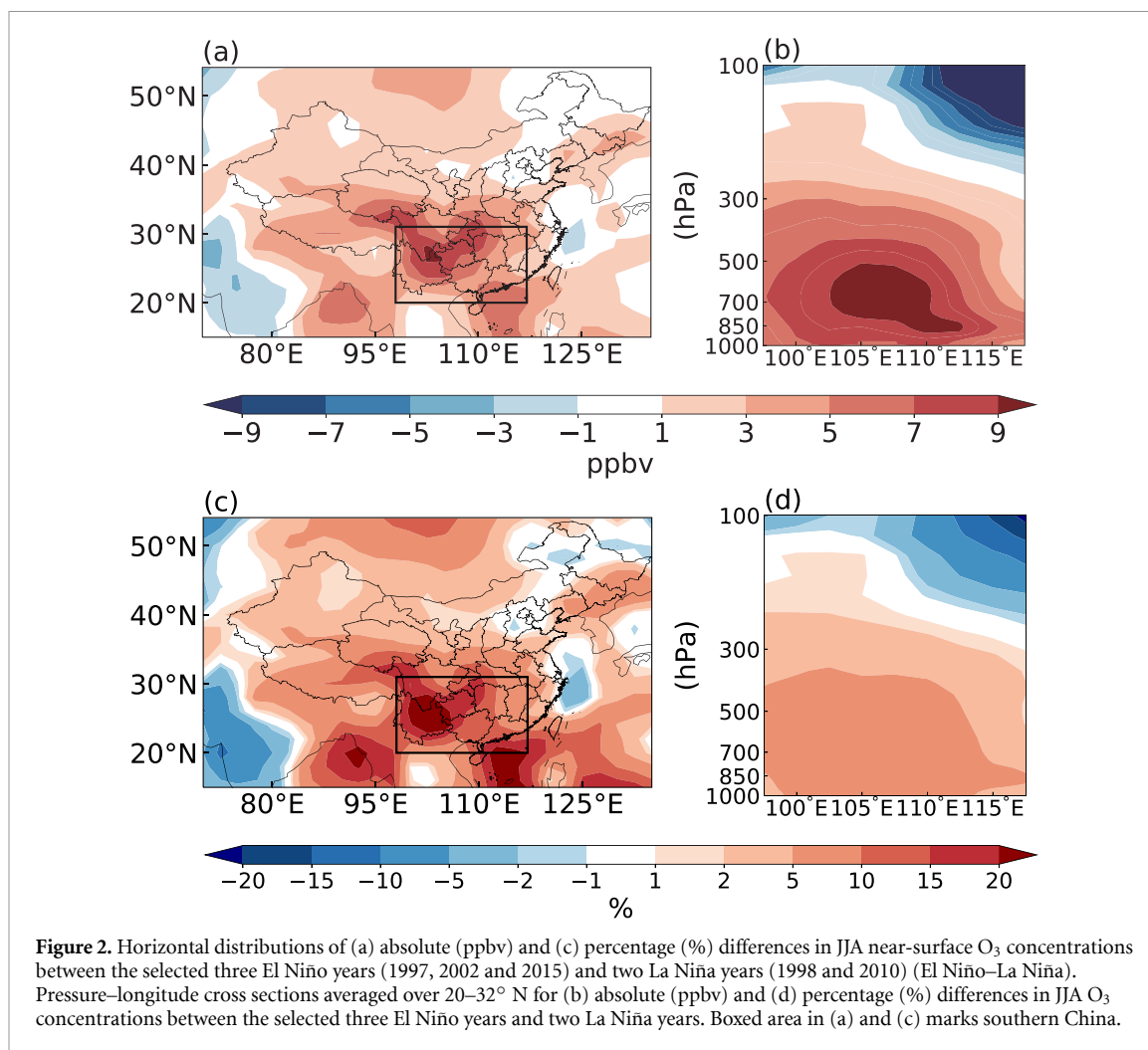
To quantitatively examine the impact of climate variabilities on air pollutants, composite differences between two opposite phases of the climate variability are commonly used in previous studies (e.g. Yang *et al* 2014). In this study, the top three strongest El Niño years (1997, 2002 and 2015) and La Niña years (1998, 1999 and 2010) during 1990–2019 are firstly selected (figure 1(b)). However, the simulated JJA near-surface  $O_3$  concentration slightly increased over southern China in the 1999 La Niña year, which is inconsistent with the positive correlation between Niño 3.4 index and  $O_3$  in China. It is likely due to the abnormal winds in JJA 1999 compared to the other two La Niña years (1998 and 2010). In general, the meridional component of winds over southern China shows anomalous northerlies during El Niño and southerlies during La Niña relative to the climatological mean (figure S3), with a correlation coefficient of  $-0.43$  between JJA Niño 3.4 index and 850 hPa meridional wind speed (figure S4). In JJA 1999, possibly dominated by other internal variabilities rather than the La Niña signal, southern China was controlled by anomalous northerlies relative to the climatological mean, leading to a different  $O_3$  transport and thus different  $O_3$  concentration changes in this particular year compared to the other two La Niña years. Therefore, we only use the other two La Niña years (1998 and 2010) in the following composite analysis.

Figure 2 shows the composite differences in JJA near-surface  $O_3$  concentrations between the selected three El Niño and two La Niña years and figure S5 gives the composite differences of the El Niño

and La Niña years compared to the climatological mean.  $O_3$  levels in the El Niño years are higher across the whole China, with the largest increases exceeding 9 ppbv (or 20% of the climatological mean) over southern China, compared to the concentrations during the La Niña years. The spatial pattern of the composite differences is identical to those of EOF (figure S1(a)) and correlation coefficients (figure 1(a)). The ENSO modulation of  $O_3$  in China is not only within the surface layer, but also extends to the middle and even upper troposphere (figures 2(b) and (d)). Averaged over the latitude range of  $20^{\circ}\text{N}$ – $32^{\circ}\text{N}$ ,  $O_3$  concentrations increase from the surface to 300 hPa during El Niño compared to La Niña years. The maximum increase by 9 ppbv (5%–10%) arises between  $105^{\circ}\text{E}$  and  $110^{\circ}\text{E}$  around 700 hPa over southern China.

#### 4. Mechanisms of ENSO impacts on $O_3$ in China

ENSO influences the chemical and physical processes of  $O_3$ , including net chemical production, horizontal advection, vertical convection, diffusion and dry deposition, through changing meteorological parameters. The role of each process can be quantified by the integrated process rate analysis to identify the dominant factors that influence the variations of  $O_3$ . The process source/sink rates are summarized in table S1. In general, JJA  $O_3$  in the troposphere over southern China is formed locally by chemical productions and dissipated due to horizontal advection, diffusion and dry deposition indicated in table S1. Figure 3 shows the composite differences in various meteorological parameters in JJA between the selected El Niño and La Niña years. Relative to La Niña years, an anomalous low at 500 hPa is located in southern China during El Niño years (figure 3(b)), which leads to a



decrease in air temperature (figures 3(d) and (g)) (Wu *et al* 2010) and is unfavorable for the O<sub>3</sub> chemical production (Gong *et al* 2019). Although the decrease in cloud cover (figure 3(c)) allows more solar radiation reaching the surface (figure 3(f)), partly compensating the less O<sub>3</sub> chemical production due to lower temperature, the net chemical production of O<sub>3</sub> in the troposphere is still lower by  $-24.8 \text{ Gg d}^{-1}$  over southern China during El Niño compared to La Niña years (table S1). Therefore, the anomalous increase in O<sub>3</sub> during El Niño years is due to the physical processes, especially the horizontal advection, which represents the only net gain ( $28.1 \text{ Gg d}^{-1}$ ) inducing the increase in O<sub>3</sub> mass in the troposphere over southern China.

In summer, meteorological fields in China are dominated by the East Asian summer monsoon, with prevailing southwesterlies over southern China. Compared to the La Niña years, southwesterlies are weakened during the El Niño years (figure 3(a)) (Zhang *et al* 2015), leading to an anomalous O<sub>3</sub> flux convergence in southern China. Table 1 summarizes the horizontal and vertical O<sub>3</sub> mass fluxes, estimated as the product of O<sub>3</sub> concentration and

wind speed, from the surface to 500 hPa, where O<sub>3</sub> concentrations have the largest change (figure 2(b)). Due to the weakened southerlies from the surface to the mid-troposphere during the El Niño years, import of O<sub>3</sub> from the south to southern China is reduced by 4.1 Tg, but the export of O<sub>3</sub> out to the north is reduced by 11.2 Tg, compared to La Niña years. The net change in meridional transport results in a O<sub>3</sub> accumulation over southern China. The bigger O<sub>3</sub> flux change in the north of southern China than in the south is due to the higher O<sub>3</sub> concentrations over land than over the coastal areas. The less import of O<sub>3</sub> from the west of southern China (1.4 Tg) and less export to the east (1.0 Tg) cause nearly no change in the zonal transport. Net upward O<sub>3</sub> transport from the lower troposphere (1.1 Tg) due to the horizontal convergence slightly restrains the surface concentration increase. Therefore, O<sub>3</sub> flux convergence is identified as the primary reason for the increase in JJA O<sub>3</sub> levels over southern China during El Niño years, relative to La Niña years.

The changes in O<sub>3</sub> over southern China in different ENSO years can be from domestic anthropogenic emissions, the transboundary transport of O<sub>3</sub> from

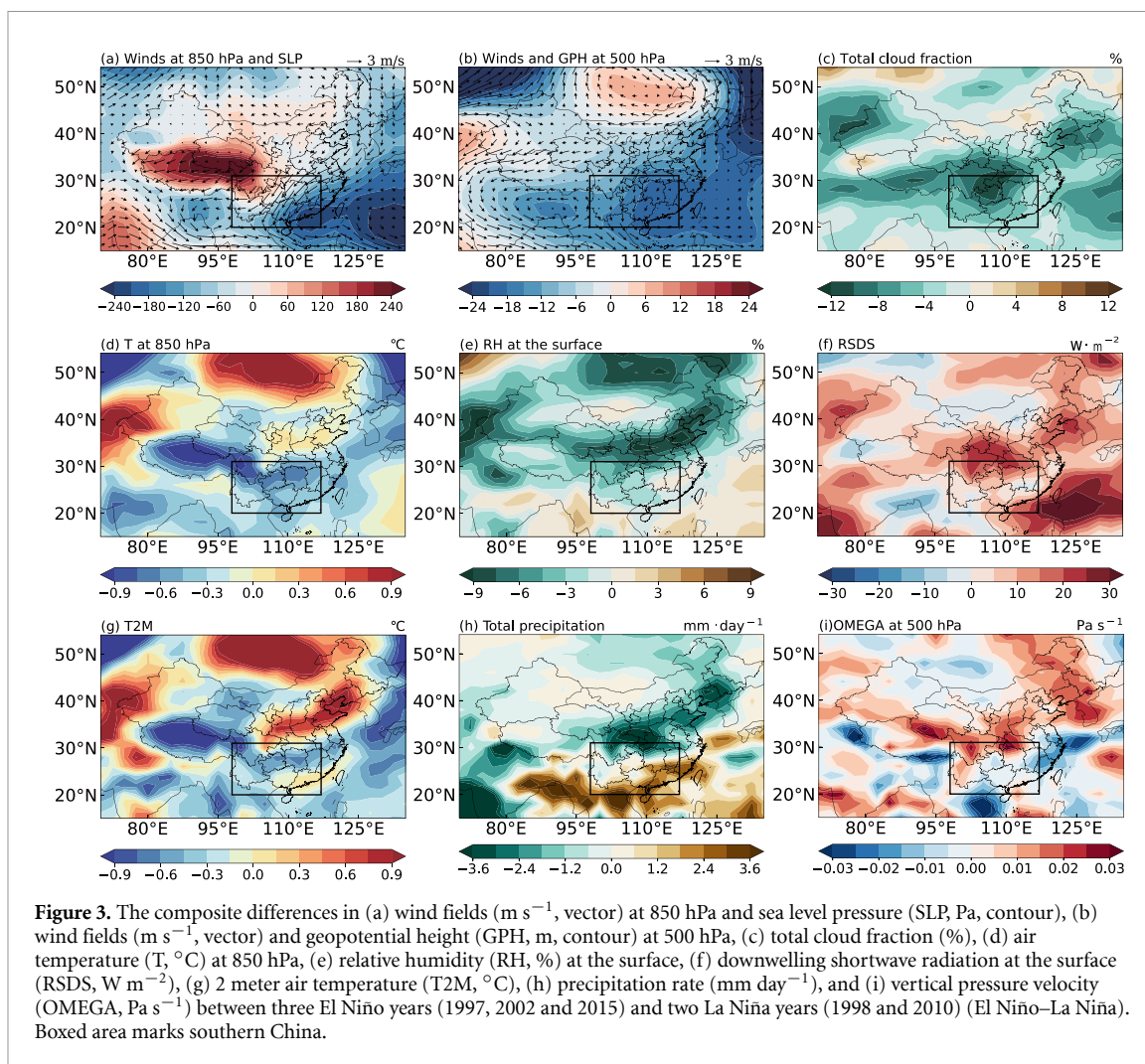
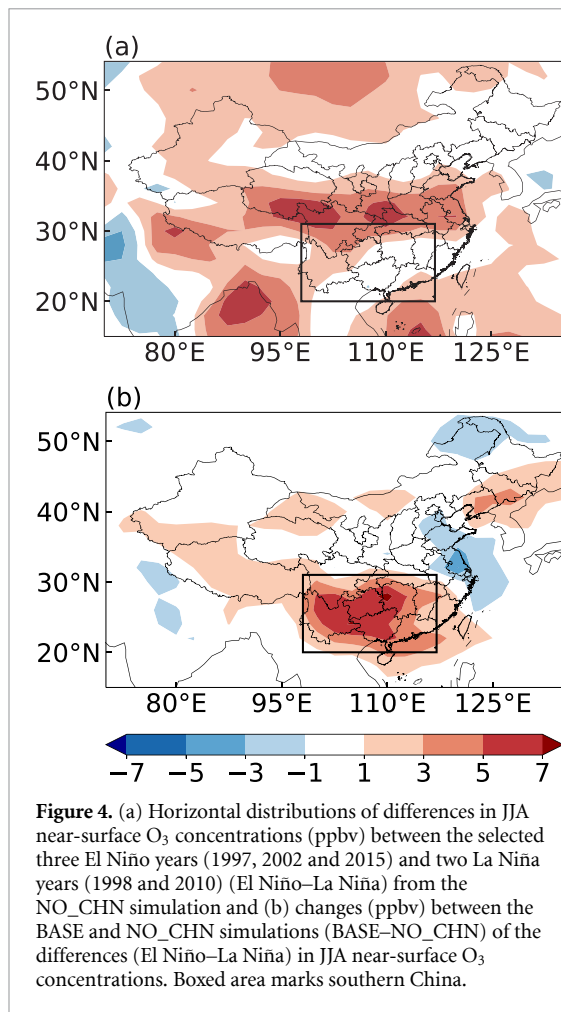


**Table 1.** The composite analyses of horizontal and vertical mass flux (Tg) of JJA  $\text{O}_3$  concentration from the surface to 500 hPa over southern China ( $97.5\text{--}117.5^{\circ}\text{ E}$ ,  $20\text{--}32^{\circ}\text{ N}$ ). The values are averaged over the selected three El Niño (1997, 2002 and 2015) and two La Niña (1998 and 2010), and the differences are also calculated (El Niño–La Niña). Positive values indicate incoming fluxes and negative values indicate outgoing fluxes.

	El Niño	La Niña	Difference
Horizontal mass flux			
East	−13.14	−14.17	1.03
West	10.36	11.76	−1.40
North	−0.09	−11.30	11.21
South	9.93	14.01	−4.08
Vertical mass flux			
Top	−8.49	−7.40	−1.09

foreign countries, the stratospheric  $\text{O}_3$  injection, or natural emissions. By turning off anthropogenic  $\text{O}_3$  precursor emissions from China in the NO\_CHN experiment, the increase in near-surface  $\text{O}_3$  concentration over southern China is much suppressed during the El Niño years (figure 4(a)). However, in NO\_CHN,  $\text{O}_3$  concentration increases in  $30\text{--}35^{\circ}\text{ E}$  latitudinal band across China, which is likely related to the variation in stratospheric  $\text{O}_3$  injection and/or

horizontal transmission and warrants in-depth analysis in future studies. About 3.8 ppbv (74% of the change in the BASE experiment) of the JJA near-surface  $\text{O}_3$  increase during the El Niño years, compared to the La Niña years, is attributed to domestic emissions (figure 4(b)). It implies that managing domestic emissions can be an effective way in mitigating  $\text{O}_3$  pollution over southern China during El Niño years.



## 5. Conclusions and discussions

Impacts of ENSO on the interannual variations of summertime near-surface O<sub>3</sub> in China over 1990–2019 are examined based on GEOS-Chem simulations, ground measurements, and MERRA-2 reanalysis data. ENSO is the crucial factor of O<sub>3</sub> variation. The near-surface O<sub>3</sub> concentration over southern China shows a positive correlation with Niño 3.4 index, but less correlations are found over northern parts of China. O<sub>3</sub> levels in El Niño years are higher over China, with the largest increases up to 20% over southern China, relative to La Niña years. The ENSO modulation of O<sub>3</sub> in China extends to the middle and upper troposphere, with the maximum impact occurring at 700 hPa over southern China. Our analysis indicates that O<sub>3</sub> flux convergence associated with the weakened southerly winds is the primary reason for the increase in JJA O<sub>3</sub> concentrations over southern China during El Niño years relative to La Niña years. In addition, O<sub>3</sub> increase over southern China during El Niño years is mainly from domestic emissions in China. We also found that the correlation coefficient between O<sub>3</sub> concentrations over southern China and CP index is much larger than EP index. This study highlights the potential significance of

ENSO in modulating O<sub>3</sub> concentrations in southern China, with great implications in O<sub>3</sub> pollution mitigation.

There are still some deficiencies and uncertainties that can be improved in future studies. Although O<sub>3</sub> observations were used to verify the simulated ENSO-induced interannual variation of O<sub>3</sub> in China, the data only cover one El Niño year during 2015–2019. Longer and continuous O<sub>3</sub> measurements spreading over China are desirable to fully explore the relationship between ENSO and O<sub>3</sub>. Figure S6 shows the observed and simulated JJA mean near-surface O<sub>3</sub> concentration anomalies in 2015, the only El Niño year during 2015–2019 (figure 1(b)), relative to the climatological averages. In summer 2015, near-surface O<sub>3</sub> concentrations increased by 3–5 ppbv (10%–12% relative to the corresponding average of 2015–2019) over southwestern China, coinciding with the maximum correlation location over China, and slightly decreased over southeastern China. It confirms that the model can simulate the ENSO-induced interannual variations in near-surface O<sub>3</sub> concentrations over China.

Additionally, natural emissions are fixed during the simulations, which can also be perturbed during the ENSO events and should be considered in future studies. Recent works have reported that, besides anthropogenic emissions, the biogenic emissions, including those from urban green spaces, exert a significant role in O<sub>3</sub> formation (Gao *et al* 2022, Ma *et al* 2022). The potential influences of fixed biogenic emissions on O<sub>3</sub> deserve further investigation. The impact of ENSO on O<sub>3</sub> is investigated in this study using the MERRA-2 driven GEOS-Chem simulations together with statistical methods. The ENSO modulation could be disturbed by other climate signals. The pure ENSO influences can be more cleanly isolated using general circulation models driven by prescribed SSTs with and without ENSO signal (Zeng *et al* 2021). The composite differences in meteorological parameters between El Niño and La Niña years from MERRA-2 reanalysis are validated here by comparing with ERA5 reanalysis (figure S7). The changes in meteorological parameters resemble each other, suggesting that MERRA-2 reanalysis is credible in representing the changes in meteorological variables during ENSO events.

## Data availability statement

The GEOS-Chem model is available at <https://zenodo.org/record/3974569#.YTD81NMzagR> (last access: 31 August 2021). MERRA-2 reanalysis data can be downloaded at <https://gmao.gsfc.nasa.gov/reanalysis/MERRA-2/> (last access: 31 August 2021). The Niño 1+2, 3, and 4 indices are downloaded from NOAA ([www.esrl.noaa.gov/psd/data/climateindices/list/](http://www.esrl.noaa.gov/psd/data/climateindices/list/), last access: 10 August 2021). The EP and CP ENSO indices can be obtained



from [10.5281/zenodo.5338939](https://zenodo.org/doi/10.5281/zenodo.5338939) (last access: 31 August 2021). Our model results are made available at [10.5281/zenodo.5338946](https://zenodo.org/doi/10.5281/zenodo.5338946) (last access: 31 August 2021).

The data that support the findings of this study are openly available at the following URL/DOI: <https://doi.org/10.5281/zenodo.5338946>.

## Acknowledgments

This study was supported by the National Natural Science Foundation of China (Grant No. 41975159) and the National Key Research and Development Program of China (Grant Nos. 2020YFA0607803 and 2019YFA0606800). H W acknowledges the support by the U.S. Department of Energy (DOE), Office of Science, Office of Biological and Environmental Research (BER), as part of the Earth and Environmental System Modeling program. The Pacific Northwest National Laboratory (PNNL) is operated for DOE by the Battelle Memorial Institute under Contract DE-AC05-76RLO1830.

## Conflict of interest

The authors declare that they have no conflict of interest.


## ORCID iDs

Yang Yang  <https://orcid.org/0000-0002-9008-5137>

Hailong Wang  <https://orcid.org/0000-0002-1994-4402>

Pinya Wang  <https://orcid.org/0000-0001-7034-7868>

Ke Li  <https://orcid.org/0000-0002-9181-3562>

Meng Gao  <https://orcid.org/0000-0002-8657-3541>

Hong Liao  <https://orcid.org/0000-0001-6628-1798>

## References

- Doherty R M *et al* 2013 Impacts of climate change on surface ozone and intercontinental ozone pollution: a multi-model study *J. Geophys. Res. Atmos.* **118** 3744–63
- Freund M B, Henley B J, Karoly D J, McGregor H V, Abram N J and Dommenges D 2019 Higher frequency of central Pacific El Niño events in recent decades relative to past centuries *Nat. Geosci.* **12** 450–5
- Fu Y, Liao H and Yang Y 2019 Interannual and decadal changes in tropospheric ozone in China and the associated chemistry-climate interactions: a review *Adv. Atmos. Sci.* **36** 975–93
- Gao M *et al* 2020 Ozone pollution over China and India: seasonality and sources *Atmos. Chem. Phys.* **20** 4399–414
- Gao Y *et al* 2022 Impacts of biogenic emissions from urban landscapes on summer ozone and secondary organic aerosol formation in megacities *Sci. Total Environ.* **814** 152654
- Gong C and Liao H 2019 A typical weather pattern for ozone pollution events in North China *Atmos. Chem. Phys.* **19** 13725–40
- Guenther A B, Jiang X, Heald C L, Sakulyanontvittaya T, Duhl T, Emmons L K and Wang X 2012 The model of emissions of gases and aerosols from nature version 2.1 (MEGAN2.1): an extended and updated framework for modeling biogenic emissions *Geosci. Model Dev.* **5** 1471–92
- Hoesly R M *et al* 2018 Historical (1750–2014) anthropogenic emissions of reactive gases and aerosols from the community emissions data system (CEDS) *Geosci. Model Dev.* **11** 369–408
- Jacob D J and Winner D A 2009 Effect of climate change on air quality *Atmos. Environ.* **43** 51–63
- Jeong J I and Park R J 2013 Effects of the meteorological variability on regional air quality in East Asia *Atmos. Environ.* **69** 46–55
- Jerrett M, Burnett R T, Pope C A 3rd, Ito K, Thurston G, Krewski D, Shi Y, Calle E and Thun M 2009 Long-term ozone exposure and mortality *New Engl. J. Med.* **360** 1085–95
- Kao H-Y and Yu J-Y 2009 Contrasting eastern-Pacific and central-Pacific types of El Niño *J. Clim.* **22** 615–32
- Kavassalis S C and Murphy J G 2017 Understanding ozone-meteorology correlations: a role for dry deposition *Geophys. Res. Lett.* **44** 2922–31
- Li K *et al* 2021 Ozone pollution in the North China Plain spreading into the late-winter haze season *Proc. Natl Acad. Sci. USA* **118** e2015797118
- Li K, Jacob D J, Liao H, Shen L, Zhang Q and Bates K H 2019 Anthropogenic drivers of 2013–2017 trends in summer surface ozone in China *Proc. Natl Acad. Sci. USA* **116** 422–7
- Lin J-T and McElroy M B 2010 Impacts of boundary layer mixing on pollutant vertical profiles in the lower troposphere: implications to satellite remote sensing *Atmos. Environ.* **44** 1726–39
- Lu K D, Guo S, Tan Z F, Wang H C, Shang D J, Liu Y H, Li X, Wu Z J, Hu M and Zhang Y H 2019a Exploring atmospheric free-radical chemistry in China: the self-cleansing capacity and the formation of secondary air pollution *Natl Sci. Rev.* **6** 579–94
- Lu X, Hong J, Zhang L, Cooper O R, Schultz M G, Xu X, Wang T, Gao M, Zhao Y and Zhang Y 2018 Severe surface ozone pollution in China: a global perspective *Environ. Sci. Technol. Lett.* **5** 487–94
- Lu X, Zhang L, Chen Y, Zhou M, Zheng B, Li K, Liu Y, Lin J, Fu T-M and Zhang Q 2019b Exploring 2016–2017 surface ozone pollution over China: source contributions and meteorological influences *Atmos. Chem. Phys.* **19** 8339–61
- Lu X, Zhang L, Wang X, Gao M, Li K, Zhang Y, Yue X and Zhang Y 2020 Rapid increases in warm-season surface ozone and resulting health impact in China since 2013 *Environ. Sci. Technol. Lett.* **7** 240–7
- Ma M *et al* 2022 Development and assessment of a high-resolution biogenic emission inventory from urban green spaces in China *Environ. Sci. Technol.* **56** 175–84
- Malley C S, Henze D K, Kuylenstierna J C I, Vallack H W, Davila Y, Anenberg S C, Turner M C and Ashmore M R 2017 Updated global estimates of respiratory mortality in adults  $\geq 30$  years of age attributable to long-term ozone exposure *Environ. Health Perspect.* **125** 087021
- Mao J Q, Paulot F, Jacob D J, Cohen R C, Crounse J D, Wennberg P O, Keller C A, Hudman R C, Barkley M P and Horowitz L W 2013 Ozone and organic nitrates over the eastern United States: sensitivity to isoprene chemistry *J. Geophys. Res. Atmos.* **118** 11256–68
- McLinden C A, Olsen S C, Hannegan B, Wild O, Prather M J and Sundet J 2000 Stratospheric ozone in 3D models: a simple chemistry and the cross-tropopause flux *J. Geophys. Res. Atmos.* **105** 14653–65
- Mills G *et al* 2018 Tropospheric ozone assessment report: present-day tropospheric ozone distribution and trends relevant to vegetation *Elementa* **6** 47

- Ni R, Lin J, Yan Y and Lin W 2018 Foreign and domestic contributions to springtime ozone over China *Atmos. Chem. Phys.* **18** 11447–69
- Olsen M A, Wargan K and Pawson S 2016 Tropospheric column ozone response to ENSO in GEOS-5 assimilation of OMI and MLS ozone data *Atmos. Chem. Phys.* **16** 7091–103
- Oman L D, Ziemke J R, Douglass A R, Waugh D W, Lang C, Rodriguez J M and Nielsen J E 2011 The response of tropical tropospheric ozone to ENSO *Geophys. Res. Lett.* **38** L13706
- Pye H O, Liao H, Wu S, Mickley L J, Jacob D J, Henze D K and Seinfeld J H 2009 Effect of changes in climate and emissions on future sulfate-nitrate-ammonium aerosol levels in the United States *J. Geophys. Res.* **114** D01205
- Qu H, Wang Y, Zhang R and Li J 2020 Extending ozone-precursor relationships in China from peak concentration to peak time *J. Geophys. Res. Atmos.* **125** e2020JD033670
- Ropelewski C F and Halpert M S 1987 Global and regional scale precipitation patterns associated with the El Niño/southern oscillation *Mon. Weather Rev.* **115** 1606–26
- Shen L and Mickley L J 2017 Effects of El Niño on summertime ozone air quality in the eastern United States *Geophys. Res. Lett.* **44** 12543–50
- Sherwen T et al 2016 Global impacts of tropospheric halogens (Cl, Br, I) on oxidants and composition in GEOS-Chem *Atmos. Chem. Phys.* **16** 12239–71
- van der Werf G R et al 2017 Global fire emissions estimates during 1997–2016 *Earth Syst. Sci. Data* **9** 697–720
- Wie J, Moon B-K, Yeh S-W, Park R J and Kim B-G 2021 La Niña-related tropospheric column ozone enhancement over East Asia *Atmos. Environ.* **261** 118575
- Wu R, Yang S, Liu S, Sun L, Lian Y and Gao Z 2010 Changes in the relationship between Northeast China summer temperature and ENSO, *J. Geophys. Res. Atmos.* **115** D21107
- Xie F, Li J, Tian W, Zhang J and Sun C 2014 The relative impacts of El Niño Modoki, canonical El Niño, and QBO on tropical ozone changes since the 1980s *Environ. Res. Lett.* **9** 064020
- Xu L, Yu J-Y, Schnell J L and Prather M J 2017 The seasonality and geographic dependence of ENSO impacts on U.S. surface ozone variability *Geophys. Res. Lett.* **44** 3420–8
- Xue L, Ding A, Cooper O, Huang X, Wang W, Zhou D and Fu C 2021 ENSO and Southeast Asian biomass burning modulate subtropical trans-Pacific ozone transport *Natl Sci. Rev.* **8** nwaa132
- Yang Y, Liao H and Li J 2014 Impacts of the East Asian summer monsoon on interannual variations of summertime surface-layer ozone concentrations over China *Atmos. Chem. Phys.* **14** 6867–79
- Yin Z, Cao B and Wang H 2019 Dominant patterns of summer ozone pollution in eastern China and associated atmospheric circulations *Atmos. Chem. Phys.* **19** 13933–43
- Yue X, Unger N, Harper K, Xia X, Liao H, Zhu T, Xiao J, Feng Z and Li J 2017 Ozone and haze pollution weakens net primary productivity in China *Atmos. Chem. Phys.* **17** 6073–89
- Zeng L, Yang Y, Wang H, Wang J, Li J, Ren L, Li H, Zhou Y, Wang P and Liao H 2021 Intensified modulation of winter aerosol pollution in China by El Niño with short duration *Atmos. Chem. Phys.* **21** 10745–61
- Zhang H, Wang Y, Park T-W and Deng Y 2017 Quantifying the relationship between extreme air pollution events and extreme weather events *Atmos. Res.* **188** 64–79
- Zhang J, Tian W, Xie F, Li Y, Wang F, Huang J and Tian H 2015 Influence of the El Niño–Southern Oscillation on the total ozone column and clear-sky ultraviolet radiation over China *Atmos. Environ.* **120** 205–16
- Zhao Z J and Wang Y X 2017 Influence of the west pacific subtropical high on surface ozone daily variability in summertime over eastern china *Atmos. Environ.* **170** 197–204
- Zheng B et al 2018 Trends in China's anthropogenic emissions since 2010 as the consequence of clean air actions *Atmos. Chem. Phys.* **18** 14095–111